Structure and physical properties of Na_4C_{60} under ambient and high pressures

Y. Kubozono,[1] Y. Takabayashi,[1] T. Kambe,[2] S. Fujiki,[1] S. Kashino,[1] and S. Emura[3]
[1]*Department of Chemistry, Okayama University, Okayama 700-8530, Japan*
[2]*Department of Physics, Okayama University, Okayama 700-8530, Japan*
[3]*ISIR, Osaka University, Osaka 567-0047, Japan*
(Received 10 April 2000; revised manuscript received 12 June 2000; published 9 January 2001)

The structure and physical properties of two-dimensional polymeric Na_4C_{60} (body-centered monoclinic, space group $I2/m$) are studied in a wide temperature region from 12 to 300 K at 1 bar, and in a pressure region up to 53 kbar at 300 K. The temperature dependence of lattice constants suggests a structural anomaly below 100 K where the variation of spin susceptibility is observed from electron spin resonance. The thermal expansion of the unit-cell volume V is smaller than that of monomeric Rb_3C_{60} and K_3C_{60}. The compressibility of c is larger than that of a and b, which can be well explained by the repulsion between Na ions. The compressibility of the center-to-center distance in the $(10\bar{1})$ plane is $\sim\frac{1}{3}$ times smaller than that in the (101) plane, which can be well explained by the formation of the polymer chains. Further, a possibility of a three-dimensional polymerization is discussed on the basis of the pressure dependence of $C_{60}\cdots C_{60}$ distances.

DOI: 10.1103/PhysRevB.63.045418 PACS number(s): 62.50.+p

I. INTRODUCTION

Recently, phases formed through a polymerization of C_{60} were discovered in metal intercalated C_{60}.[1–17] First, AC_{60} (A=K, Rb, and Cs) forms a one-dimensional (1D) polymer between C_{60} molecules through [2+2] cycloaddition to lead a four-membered ring.[1–8] AC_{60} shows interesting properties characteristic of 1D organic conductors. The polymer phases of RbC_{60} and CsC_{60} are metallic above 50 K, and transform to an insulating state below 50 K. The electron spin resonance (ESR) shows that the transition is based on the instability of the 1D metal through a spin-density-wave.[4–8] Second, a metastable phase of AC_{60} forms a $(C_{60})_2^{2-}$ dimer with a single C-C bond.[4,7–12] This phase is realized by quenching fcc AC_{60} from 500 K to temperatures below 270 K. ESR and optical studies suggested a diamagnetic insulating ground state for the metastable phase of AC_{60}.[9,10,13] Third, Na_2RbC_{60} forms a 1D polymer of C_{60} connected by a single C-C bond.[14,15] It is known that Na_2RbC_{60} is a cubic fullerene superconductor with superconducting transition temperature (T_C) of 3.4 K at 1 bar, and loses cubic symmetry at a modest pressure below 3 kbar.[16] Recently, Bendele *et al.* found that Na_2RbC_{60} loses its cubic symmetry and forms a 1D polymer with the single C-C bonds when cooling slowly to temperatures below 230 K.[14,15] This transition was confirmed by ^{13}C and ^{23}Na NMR experiments.[17] Fourth, Na_4C_{60} forms a 2D polymeric phase with a body-centered-monoclinic (bcm) structure of space group $I2/m$. In this phase, the C_{60} molecules are connected through single C-C bonds in the $(10\bar{1})$ plane.[18] This phase exhibits a metallic behavior, contrary to other insulating A_4C_{60} phases,[19–22] and transforms to a monomeric phase (body-centered-tetragonal (bct):$I4/mmm$) at 500 K,[23] whose structure is the same as those of K_4C_{60} and Rb_4C_{60}.[24,25] ESR shows that this phase transition is a metal-metal transition.[23] The metallic behavior of Na_4C_{60} can be reasonably explained by smaller lattice constants than those of the other A_4C_{60}, which are understood as the nonmagnetic molecular Jahn-Teller Mott insulator.[26,27] Further, the temperature dependence of spin susceptibility χ_{spin} of Na_4C_{60} estimated from ESR shows a transformation from temperature-independent (Pauli-like) behavior to a rapidly increasing one below 100 K, and a further rapidly decreasing one below 20 K.[18]

The first purpose of the present study is to search for a structural transition below 100 K from the temperature dependence of the x-ray diffraction of Na_4C_{60} at 1 bar, in order to clarify the origin of the magnetic transition. The second purpose is to search for phases in Na_4C_{60} under pressure and to study the structures and physical properties of 2D polymeric Na_4C_{60} under pressure.

II. EXPERIMENT

The Na_4C_{60} sample was prepared by annealing stoichiometric amounts of C_{60} and Na metal for 100 h at 723 K under a vacuum of 10^{-5} Torr; a trace of benzene contained in C_{60} powder was removed before annealing. The sample was introduced into a glass capillary for Raman and x-ray-diffraction measurements at 1 bar, into diamond-anvil cells for x-ray-diffraction measurements under pressure, and into a quartz tube for ESR measurement at 1 bar. ESR spectra were recorded from 290 to 16 K with a Bruker ESP300 ESR spectrometer. The temperature was regulated within ± 1 K with an Oxford He flow Cryostat (ESR910). The spin susceptibility χ_{spin} was determined by comparing the integrated intensity of the ESR for the sample with that for $CuSO_4 5H_2O$ ($\chi_{spin}=6.00\times10^{-6}$ emu/g at 290 K).[28] The raman spectrum was measured by using an ISA Confocal LABRAM system at an excitation of 632.8 nm with a He-Ne laser. The x-ray-diffraction pattern was measured with synchrotron radiation at the BL-1B in the Photon Factory of High Energy Accelerator Research Organization (KEK-PF). The wavelengths λ used for the x-ray-diffraction measurements were 1.1002(2) Å in a temperature region below 300 K at 1 bar, and 0.6904(1) Å in a pressure region from 1 bar to 53 kbar at 300 K.

III. RESULTS AND DISCUSSION

Figures 1(a) and 1(b) show a Raman peak for a C_{60} intramolecular Ag(2) mode, and an x-ray-diffraction pattern at

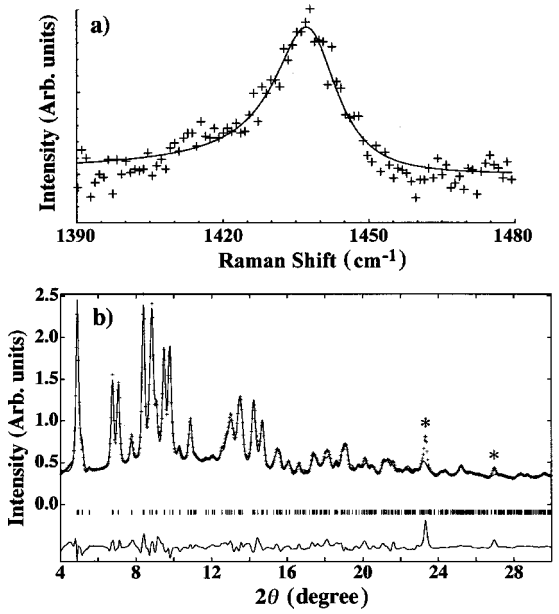

FIG. 1. (a) Raman peak of the C_{60} intramolecular Ag(2) mode, and (b) the x-ray-diffraction pattern at 300 K under a pressure of 1 bar [$\lambda = 0.6904(1)$ Å]. The observed data are denoted by the data points (+ symbols), and the calculated plots are by the solid lines. In (b), the allowed peak positions and the difference between the observed and calculated patterns are drawn by ticks and the solid line, respectively. Two peaks due to the sample holder are shown by asterisks. In the Rietveld refinement shown in (b), the final weighted pattern R factor $R_{wp} = 0.061$, the final integrated intensity R factor $R_I = 0.024$, and the goodness of fit $S = 1.7$; S is the ratio of R_{wp} to the expected R factor, R_{exp}, and a measure of the adequacy of the model used in the refinement.

300 K, respectively. The Raman peak at 300 K shows a center frequency ω_0 of 1438 cm^{-1} and a linewidth Γ of 8 cm^{-1}. ω_0 shows that this sample is Na_4C_{60} because one-electron transfer to C_{60} results in a redshift of 7 cm^{-1} from ω_0 in the Ag(2) Raman peak of pristine C_{60}: 1467 cm^{-1}.[29] The x-ray-diffraction pattern at 300 K shows a pattern characteristic of the polymeric phase of Na_4C_{60} (bcm, $I2/m$, $Z = 2$).[18]

The x-ray-diffraction pattern was analyzed according to the procedure reported by Oszlanyi *et al.*[18] First, the Cartesian coordinates of 60 C atoms in a C_{60} molecule were generated under the $m3$ point-group symmetry from the coordinates of three C atoms shown in Ref. 18. Second, the C_{60} molecule was rotated by Eulerian angles of $\psi = -55.3°$, $\theta = 25.8°$, and $\phi = 49.1°$. Third, the coordinates were transferred into fractional atomic coordinates for the monoclinic lattice, where the a, b, c, and β reported in Ref. 18 were employed; the C_{60} molecule is centered on the origin of the unit cell. Fourth, the coordinates of independent 30 C atoms were chosen in the $I2/m$ lattice, where a disordered C_{60} molecule related by a twofold rotation axis along b was automatically formed by the symmetry operations of the $I2/m$; the Eulerian angles are $\psi = -124.7°$, $\theta = 154.2°$, and $\phi = -130.9°$. As reported by Oszlanyi *et al.*,[18] it is difficult to distinguish the space groups of $I2/m$ and $P21/n$ based on the x-ray powder diffraction pattern. Consequently, we adopted the space group $I2/m$ in the analysis of x-ray-diffraction pattern according to Oszlanyi *et al.* The Na ions were located at $4h$ and $4i$. The Rietveld refinement was performed by using a RIETAN 94 program.[30] The lattice constants a, b, c, and β, were determined to be 11.24(1), 11.71(1), 10.25(1) Å, and 96.08(4)°, respectively, in good agreement with those reported previously.[18] The occupancy factors of the Na atoms at $4h$ and $4i$ were 0.99(3) and 0.92(2), respectively. Therefore, the sample used in this study is $Na_{3.82(7)}C_{60}$, comparable to the sample used by Oszlanyi *et al.*, $Na_{3.72(8)}C_{60}$.[18] In this analysis, the isotropic displacement parameter B for Na and C atoms were fixed to the previous ones.[18] The atomic coordinates of C atoms were not refined, but these were adjusted to the new a, b, c, and β to maintain the first molecular geometry. Though we tried to determine the exact C_{60} geometry by taking into account the distortion of C_{60} mol-

TABLE I. Structural parameters from Rietveld analysis for Na_4C_{60} at 1 bar and 300 K. The space group is $I2/m$. The lattice parameters are $a = 11.24(1)$, $b = 11.71(1)$, and $c = 10.25(1)$ Å, and $\beta = 96.08(4)°$. The final weighted pattern R factor $R_{wp} = 0.061$, and the final integrated intensity R factor $R_I = 0.024$.

	Site	x	y	z	Occupancy	B (Å^2)
Na1	$4h$	0.5	0.205(3)	0	0.99(3)	5
Na2	$4i$	0.696(4)	0	0.465(3)	0.92(2)	5
C1	$8j$	0.1640	0.1096	0.2877	0.5	2
C2	$8j$	0.0486	0.1031	0.3268	0.5	2
C3	$8j$	0.2752	0.0719	−0.1198	0.5	2
C4	$8j$	0.2983	−0.0396	−0.0747	0.5	2
C5	$8j$	−0.0361	0.2984	−0.0504	0.5	2
C6	$8j$	−0.0789	0.2556	−0.1741	0.5	2
C7	$8j$	0.2621	0.1634	−0.0271	0.5	2
C8	$8j$	−0.1904	−0.0917	0.2343	0.5	2
C9	$8j$	−0.3092	0.0635	−0.0649	0.5	2
C10	$8j$	0.2375	−0.1352	−0.1423	0.5	2
C11	$8j$	0.0901	0.2903	−0.0048	0.5	2
C12	$8j$	0.1032	−0.2794	−0.0608	0.5	2
C13	$8j$	−0.0030	−0.2032	0.2564	0.5	2
C14	$8j$	−0.1904	0.1923	−0.1909	0.5	2
C15	$8j$	0.1907	0.1926	0.1900	0.5	2
C16	$8j$	−0.2295	−0.0059	−0.2657	0.5	2
C17	$8j$	0.0442	−0.1794	−0.2696	0.5	2
C18	$8j$	−0.0054	−0.0074	0.3453	0.5	2
C19	$8j$	0.2726	0.1403	0.1076	0.5	2
C20	$8j$	−0.1317	0.0007	0.2996	0.5	2
C21	$8j$	−0.2966	−0.0248	−0.1544	0.5	2
C22	$8j$	0.1556	−0.1161	−0.2529	0.5	2
C23	$8j$	0.1693	0.2397	−0.0843	0.5	2
C24	$8j$	0.2109	−0.2183	−0.0447	0.5	2
C25	$8j$	−0.1249	−0.1954	0.2123	0.5	2
C26	$8j$	−0.2552	0.1740	−0.0834	0.5	2
C27	$8j$	0.1010	0.2663	0.1348	0.5	2
C28	$8j$	−0.1773	0.1008	−0.2836	0.5	2
C29	$8j$	0.0185	−0.2596	−0.1753	0.5	2
C30	$8j$	0.0578	−0.1076	0.3241	0.5	2

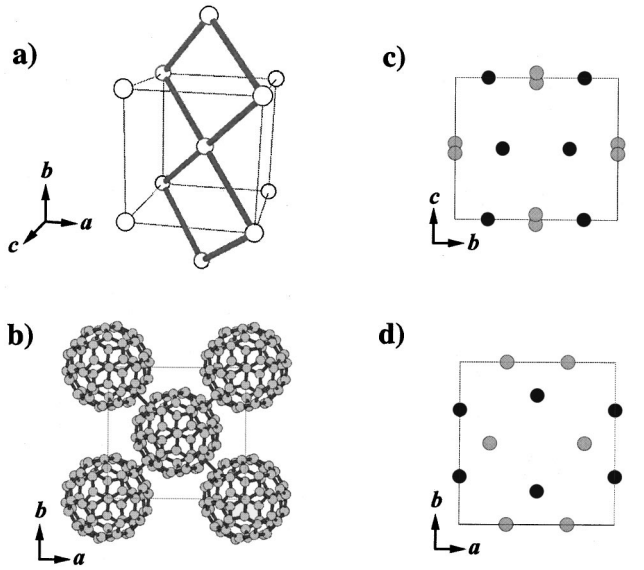

FIG. 2. (a) The bcm unit cell, and (b) the view along the [001] direction of the unit cell; C_{60} molecules are denoted by white balls in (a) and by C atoms in (b). (c) [100] and (d) [001] projections of the unit cell; Na atoms are denoted by balls. The black and gray balls refer to the Na atoms at $4h$ and $4i$, respectively.

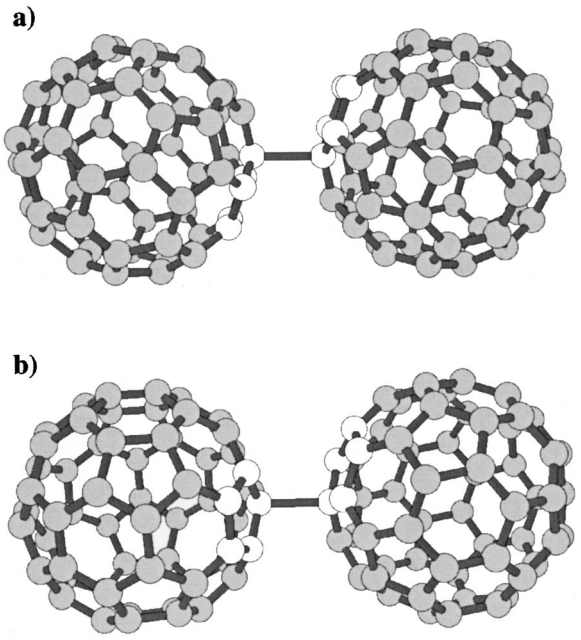

FIG. 3. The chain units formed between the C_{60} molecules with (a) the same configuration and (b) different orientations. The white balls refer to the pentagon ring which contains the bonding C atoms.

ecule from I_h symmetry, it was difficult to determine it based on x-ray powder diffraction. Consequently, the lowering in the molecular symmetry of C_{60} was not taken into account in this analysis. Finally, for Na atoms, y at $4h$, and x and z at $4i$ were refined. The final structural parameters are listed in Table I.

Figures 2(a) and 2(b) show the bcm unit cell of Na_4C_{60}. The position of C_{60} molecules are denoted by small white balls in Fig. 2(a). The arrangement of the C_{60} molecules viewed along the [001] is shown in Fig. 2(b). The polymer chains are formed along the $\langle 111 \rangle$ directions in the $(10\bar{1})$ plane. The nearest center-to-center distance between the C_{60} molecules is 9.28(1) Å, which is slightly larger than those for 1D polymeric AC_{60} formed by [2+2] cycloaddition (9.14 Å for RbC_{60} and 9.11 Å for KC_{60}).[3,4] However, the distance in Na_4C_{60} is slightly smaller than that in AC_{60} dimer and Na_2RbC_{60} polymer phases with a single C-C bond [9.34 Å for RbC_{60} and KC_{60},[4,12] and 9.35 Å for Na_2RbC_{60} (Ref. 14)]. The center-to-center distance between C_{60} molecules along the $\langle 111 \rangle$ directions in the (101) plane is 9.91(1) Å, which implies van der Waals contacts. The value is smaller than that of monomeric Na_2C_{60}[10.03(1) Å] (Refs. 31 and 32) and C_{60}(10.02 Å).[33]

Figures 2(c) and 2(d) show the [100] and [001] projections, respectively, of the bcm unit cell in which Na atoms at $4h$ and $4i$ are denoted by black and gray balls, respectively. The first nearest distance between Na atoms, 4.54(8) Å, is found between the Na atoms at $4i$ in the (010) plane. The value is close to the sum of van der Waals radius (2.27 Å) (Ref. 34) of the Na atom. The second-nearest Na···Na distance is 4.81(7) Å between Na atoms at $4h$ in the (100) plane. The bonds formed between the C_{60} molecules are shown for two possible orientations in Figs. 3(a) and 3(b). The C···C distance between C_{60} molecules is 2.18 Å for both orientations. The long C-C distance is caused because the distortion of C_{60} molecule is not taken into account in this Rietveld refinement. If the exact C_{60} geometry can be determined, the C-C distance would become short as that determined in the Na_2RbC_{60} polymer phase, ~1.7 Å.[35] The molecular conformations around the C···C bonds are reasonable for both orientations. These results mean that the polymer chain can be formed between the C_{60} molecules with two possible orientations which are randomly distributed with 50% probability in the unit cell. The first and the second nearest C···C distances between the C_{60} molecules in the (101) plane are 3.24 and 3.26 Å, respectively, for the same orientation while 3.01 and 3.20 Å for the different orientation. These values are comparable to the first nearest C···C distances in the monomeric Na_2C_{60}(3.15 Å),[31] K_3C_{60}(3.14 Å),[24] Rb_3C_{60}(3.32 Å),[24] and C_{60}(3.15 Å).[24,36]

The ESR spectra were analyzed by a least-squares fitting with a single Lorentzian function from 16 to 290 K. The χ_{spin}, the peak-to-peak linewidth ΔH_{pp}, and the g factor were estimated to be 1.4×10^{-4} emu/mol, 1.7 G, and 2.0012 at 290 K, respectively. The value of χ_{spin} is consistent with that reported previously, 1.7×10^{-4} emu/mol.[18] The density of state $N(\varepsilon_F)$ is 2 state/eV-spin-C_{60}, suggesting a broad bandwidth. $N(\varepsilon_F)$ is smaller than the densities of states of monomeric fullerides (14 state/eV-spin-C_{60} for K_3C_{60} and 19 state/eV-spin-C_{60} for Rb_3C_{60}).[37] The broad bandwidth in Na_4C_{60} can be explained by the small C_{60}-C_{60} distance due to the formation of the polymer chain. However, the $N(\varepsilon_F)$ of Na_4C_{60} is smaller than that of the polymeric Na_2RbC_{60} with single C-C bonds (11 state/eV-spin-C_{60} from $\chi_{spin}=9.5\times10^{-4}$ emu/mol).[38] Though the center-to-center distance between C_{60} molecules is almost the same between Na_4C_{60} and

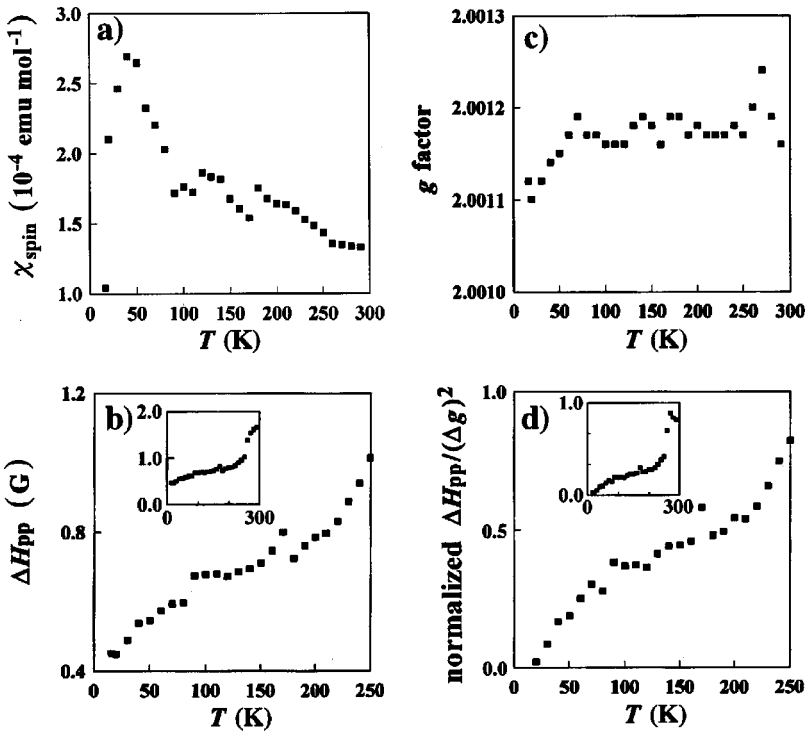

FIG. 4. Plots of (a) χ_{spin}, (b) ΔH_{pp}, (c) the g factor, and (d) $\Delta H_{\mathrm{pp}}/(\Delta g)^2$ vs temperature.

Na_2RbC_{60}, as described previously, two dimensionality in Na_4C_{60} may result in band broadening, i.e., samll $N(\varepsilon_F)$.

Figures 4(a), 4(b), 4(c), and 4(d) show the temperature dependence of the χ_{spin}, ΔH_{pp}, g factor, and $\Delta H_{\mathrm{pp}}/(\Delta g)^2$, respectively: $\Delta g = g - 2.0023$. The χ_{spin} shows a slight decrease with an increase in temperature above 100 K, suggesting that the phase is metallic (a Pauli-paramagnetic state). The χ_{spin} increases rapidly with a decrease in temperature from 80 to 40 K, and decreases abruptly below 40 K. Such a temperature dependence can also be found in a figure (Fig. 4) of Ref. 18 though Oszlanyi *et al.* did not comment on it. The values of ΔH_{pp} and $\Delta H_{\mathrm{pp}}/(\Delta g)^2$ decrease rapidly when decreasing temperature from 300 to 200 K [see the insets of Figs. 4(b) and 4(c)], and decrease slightly with a decrease in temperature from 200 to 100 K. Further, slopes of the plots of ΔH_{pp} and $\Delta H_{\mathrm{pp}}/(\Delta g)^2$ versus temperature change at 100 K. The g factor is constant above 80 K, and shows a rapid decrease below 100 K. These results suggest a transition of the Pauli-paramagnetic state below 100 K. The temperature dependence of ΔH_{pp} below 100 K is different from that of the 1D polymeric phase of RbC_{60}, in which ΔH_{pp} increases rapidly with a decrease in temperature below the transition temperature (50 K).[5] The ground state in RbC_{60} is interpreted as an antiferromagnetic state, like that below 30 K in CsC_{60}.[5,39,40] On the other hand, the transition observed in Na_4C_{60} may be attributed to the charge-density-wave (CDW)-type dimerization (spin singlet) because the temperature dependence of χ_{spin} and ΔH_{pp} decreases rapidly with a decrease in temperature below 50 K. A (spin-Peierls) nonmagnetic ground state is realized below 13.8 K in the 1D polymeric CsC_{60}, and the nonmagnetic state coexists with the magnetic ordered state which is realized below 30 K.[39] If

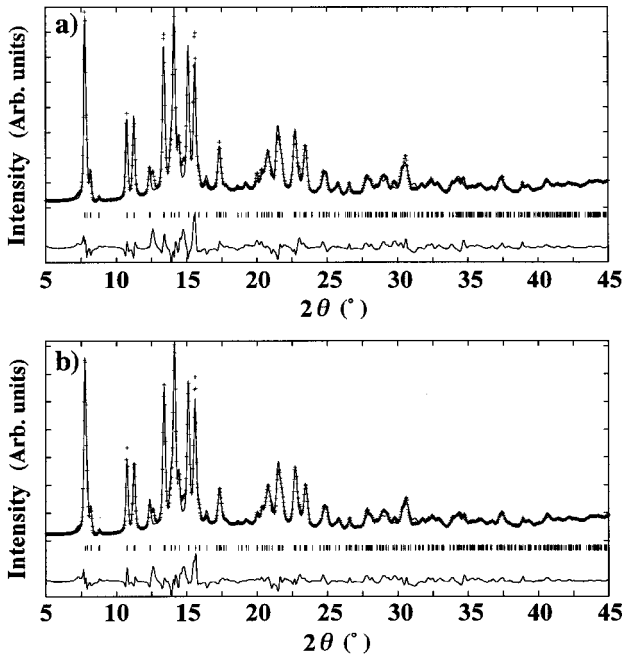

FIG. 5. X-ray-diffraction patterns at (a) 70 K and (b) 12 K under a pressure of 1 bar [$\lambda = 1.1002(2)$ Å]. The observed data are denoted by the data points (+ symbols), and the calculated plots are by the solid lines. The weak peak at ~12.5° found in (a) and (b) was assigned to pristine C_{60}(<5%). The pristine C_{60} was found only in a batch used for temperature-dependent x-ray-diffraction measurement. The allowed peak positions and the difference between the observed and calculated patterns are drawn by ticks and solid lines, respectively. $R_{\mathrm{wp}} = 0.089$, $R_I = 0.036$, and $S = 1.8$ at 70 K, and $R_{\mathrm{wp}} = 0.086$, $R_I = 0.028$, and $S = 1.7$ at 12 K.

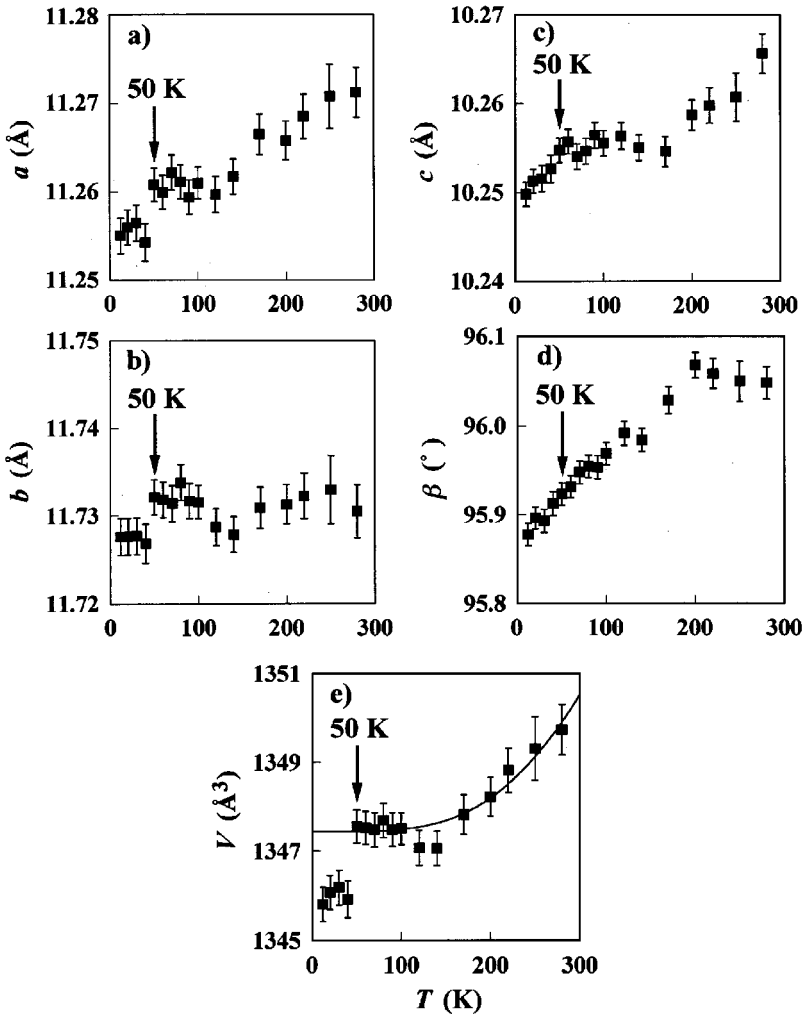

FIG. 6. Plots of (a) a, (b) b, (c) c, (d) β, and (e) V vs temperature. The curve calculated with the Grüneisen relation within the Debye approximation is shown in (e).

the transition in Na_4C_{60} can be assigned to CDW-type dimerization through the electron-phonon interaction, the structural change may be observed around 50 K. Recently, a structural anomaly was observed around 14 K in CsC_{60}.[40]

Figures 5(a) and 5(b) show x-ray-diffraction patterns at 70 and 12 K as typical examples observed in a low-temperature region at 1 bar. The x-ray-diffraction patterns were analyzed according to the same procedure as that at 300 K, except for that B's for Na atoms were refined. All x-ray-diffraction patterns from 12 to 280 K can be indexed with $I2/m$. The temperature dependence of a, b, c, and β, and the unit-cell volume V, are shown in Figs. 6(a)–6(e). The temperature dependences of a, b, and V show a discontinuity at 50 K which corresponds to the temperature exhibiting the maximum in $\chi_{\rm spin}$. The plots of c also show a decrease below 50 K. These results are similar to those observed for lattice constants in the 1D polymeric phase of CsC_{60}.[40] The structural anomaly observed below 14 K for CsC_{60} is interpreted as an indication of a spontaneous strain which appears along the polymer chain axis and the interchain direction. Further, the strain was related to the appearance of a nonmagnetic state and magnetoelastic coupling between the localized spin on C_{60} and the (spin-Peierls) phonon degrees of freedom. The anomaly of the lattice constants observed in Na_4C_{60} around 50 K may also be assigned to such a spontaneous strain that is expected in CDW-type dimerization. Therefore, this structural anomaly may be related to a transition from the Pauli-paramagnetic state suggested by ESR. Plots of b, c, and V in Na_4C_{60} show a small and continuous increase with a decrease in temperature below 100 K. To confirm the discontinuous variation of V around 50 K, curve fitting was performed by a Grüneisen relation within the Debye approximation [Fig. 6(e)]. V below 50 K could not be fitted by the Grüneisen relation, as seen from Fig. 6(e). This also suggests a structural change around 50 K. However, β decreases monotonically with a decrease in temperature in the temperature region below 200 K. Further, new Bragg reflections were not found below 100 K, as in Cs_3C_{60}.[40] Consequently, these data do not allow one to conclude the structural transition around 50 K clearly. Further study on the structure in the low-temperature region should be performed by single-crystal x-ray diffraction and neutron diffraction.

Negative thermal expansion below 100 K can result in an increase in $N(\varepsilon_F)$ with a decrease in temperature because of the decrease in the transfer integral t between the C_{60} molecules, leading to an increase in $\chi_{\rm spin}$. However, the large increase in $\chi_{\rm spin}$ observed in ESR from 80 to 40 K cannot be explained by such a lattice expansion, because the difference

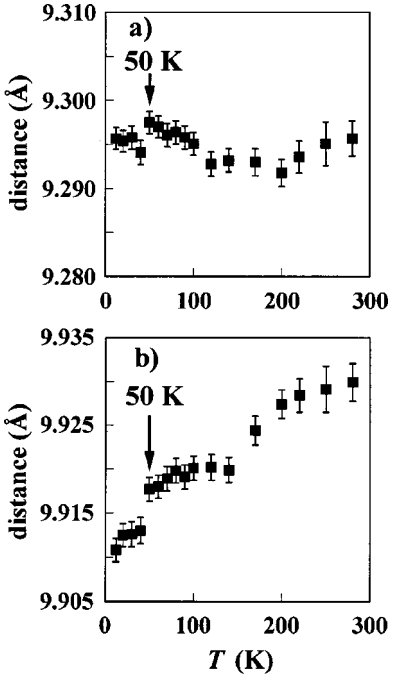

FIG. 7. Plots of the center-to-center distance between the C_{60} molecules in (a) $(10\bar{1})$ and (b) (101) planes vs the temperature.

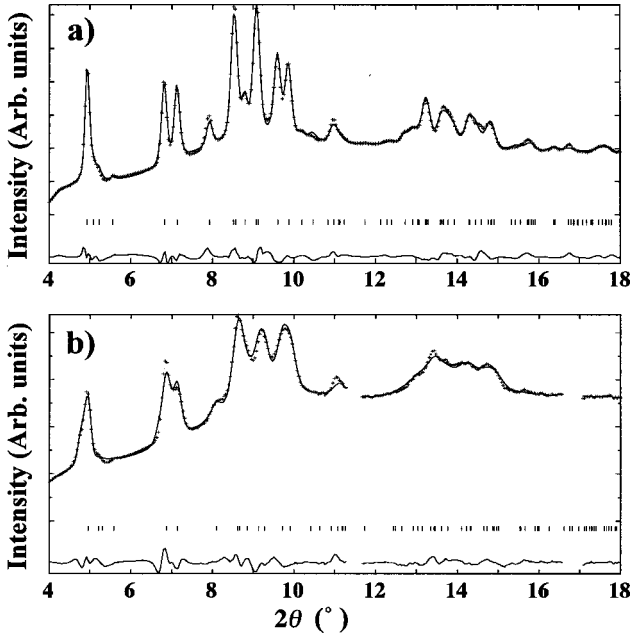

FIG. 8. X-ray-diffraction patterns at 300 K under pressures of (a) 22 kbar and (b) 51 kbar [$\lambda = 0.6904(1)$ Å]. The peak originating from the diamond anvil cell was eliminated in (b). The observed data are denoted by the data points (+ symbols), and the calculated plots are by solid lines. The allowed peak positions and the difference between the observed and calculated patterns are drawn by ticks and solid lines, respectively. $R_{wp} = 0.025$, $R_I = 0.005$, and $S = 1.6$ at 22 kbar, and $R_{wp} = 0.024$, $R_I = 0.006$, and $S = 1.6$ at 51 kbar.

in V between 50 and 120 K is very small [1347.6(4) Å^3 for V at 50 K and 1347.1(4) Å^3 at 120 K].

The plots of the center-to-center distances between C_{60} molecules in the $(10\bar{1})$ and (101) planes are shown in Figs. 7(a) and 7(b). The center-to-center distance in the $(10\bar{1})$ plane, which is associated with the polymer chain, increases slightly with an increase in temperature above 200 K, and is constant from 120 to 200 K. Further, the value increases with a decrease in temperature below 120 K, and shows a maximum at 50 K. The value at 50 K is larger than that at 280 K. The value shows a discontinuous and rapid decrease at 40 K. On the other hand, the center-to-center distance in the (101) plane shows a large increase above 140 K and a discontinuous and rapid decrease at 40 K. These results also reflect the structural anomaly below 100 K. The center-to-center distances between the C_{60} molecules in the $(10\bar{1})$ and (101) planes at 12 K are 9.296(1) and 9.911(1) Å, respectively. Further, β does not reach 90° even at 12 K [$\beta = 95.88(1)°$ at 12 K]. These results imply that the possibility of the 3D polymerization can be neglected in the temperature region studied at 1 bar.

Figures 8(a) and 8(b) show x-ray-diffraction patterns under pressures of 22 and 51 kbar, respectively, at 300 K, which can be indexed with $I2/m$ as in the x-ray-diffraction pattern at 1 bar. All x-ray-diffraction patterns under pressure were analyzed according to the same procedure as that at 1 bar, except for that B's for Na atoms were refined. The pressure dependence of a, b, c, β, and V are shown in Figs. 9(a)–9(e). The linear compressibility κ was determined for Na_4C_{60} because the linear extrapolation is applicable for the pressure dependence of the lattice constants in the pressure region below 53 kbar studied here. The κ's of a [$2.16(1) \times 10^{-4}$ kbar^{-1}], b [$3.38(2) \times 10^{-4}$ kbar^{-1}], and c [$8.8(1) \times 10^{-4}$ kbar^{-1}] in Na_4C_{60} are smaller than those of monomeric fullerenes [1.7×10^{-3} kbar^{-1} for Na_2C_{60},[41] $1.20(9) \times 10^{-3}$ kbar^{-1} for K_3C_{60},[42] $1.52(9) \times 10^{-3}$ kbar^{-1} for Rb_3C_{60},[42] and $2.3(2) \times 10^{-3}$ kbar^{-1} or 2.7×10^{-3} kbar^{-1} for C_{60} (Refs. 42–44)]. Further, the κ of V of Na_4C_{60} [$1.37(3) \times 10^{-3}$ kbar^{-1}], is smaller than the κ's of Na_2CsC_{60} (6.4×10^{-3} kbar^{-1})[45] and Li_3CsC_{60} (2.6×10^{-3} kbar^{-1}),[46] which polymerize through 1D C-C single bonds. It can be deduced as a first approximation that the values of κ in Na_4C_{60}, smaller than those of monomeric and 1D polymeric fullerenes, originate from the formation of the 2D polymer chains.

The κ of c in Na_4C_{60} is larger than the κ's of a and b. The small κ of b may be ascribed to the formation of a polymer chain. However, the difference in κ between c and a cannot be explained by the formation of polymer chains between C_{60} molecules because the effect contributes almost equally to a and c. The small κ of a can be ascribed to the close Na···Na contact along the [100] direction in the (010) plane [4.54(8) Å at 1 bar and 300 K]. The Na···Na distance along the [001] direction [10.25(8) Å at 1 bar and 300 K] is twice as large as that along the [100] direction. Thus the small repulsion between Na atoms along the [001] direction results in the large κ of c. Further, the second close Na···Na distance along the [010] direction [4.81(7) Å at 1 bar and 300 K] can contribute to the small κ of b. In fact, the values of κ increase with an increase in the Na···Na distance. On the other hand, the closest Na···C distances between the Na

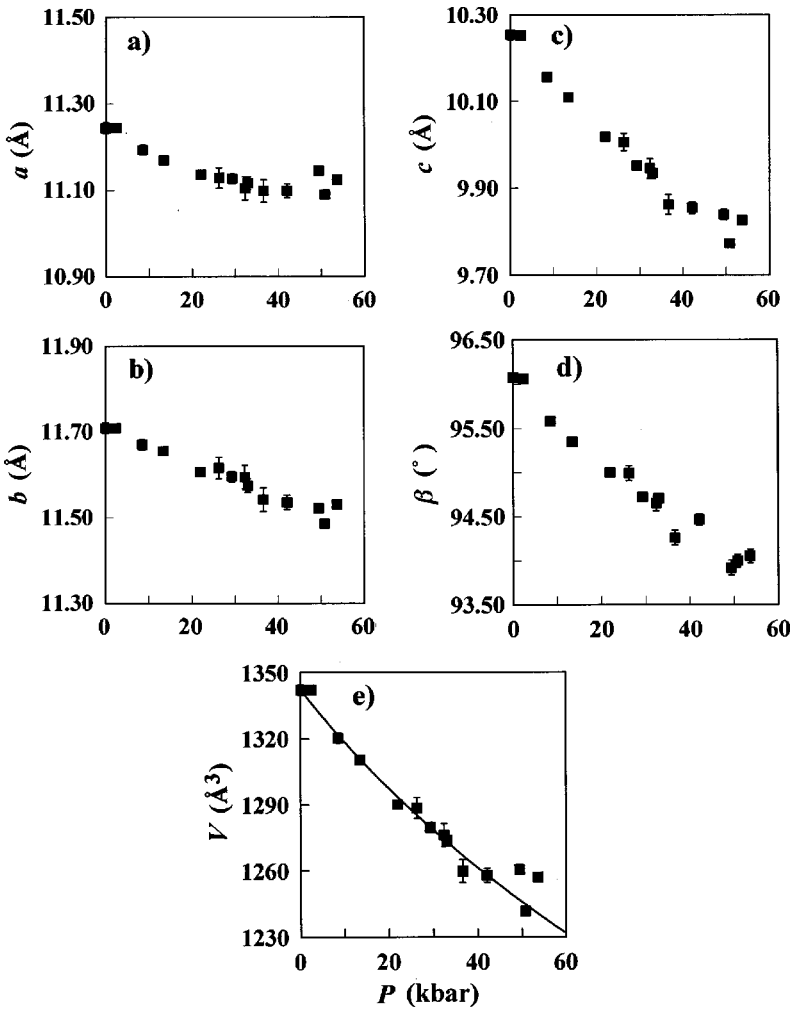

FIG. 9. Plots of (a) a, (b) b, (c) c, (d) β, and (e) V vs pressure. The fitting curve with the Murnaghan EOS is shown in (e).

atom and the C_{60} molecule along the [100], [010] and [001] directions are 2.80(4), 2.70(4) and 2.71(4) Å, respectively, at 300 K under a pressure of 1 bar. These values are close to the sum of the ionic radius of Na^+ (1.16 Å for a coordination number of 6),[47] and the van der Waals radius of the C atom (1.70 Å).[34] The difference in the Na···C distance cannot be related to the difference in the κ of a, b, and c.

The pressure dependence of the Na···Na distance in the (010) plane is shown in Fig. 10(a). The Na···Na distance shows a substantial linear decrease with an increase in pressure up to 53 kbar. The distance is 3.8(2) Å at 49 kbar, which is larger than that of the Na_9 cluster in $Na_{11}C_{60}$, 2.78 Å.[48] Figure 10(b) shows the pressure dependence of the center-to-center distances between the neighboring C_{60} molecules in the $(10\bar{1})$ and (101) planes. The distances in the $(10\bar{1})$ and (101) planes are dominated by the chemical bond forming the polymer chains and the van der Waals contacts between the C_{60} molecules, respectively. The distance in the (101) plane shows a rapid decrease in comparison with that in the $(10\bar{1})$ plane. κ of the center-to-center distance between the C_{60} molecules in the $(10\bar{1})$ plane $[2.11(1)\times10^{-4}\,\mathrm{kbar}^{-1}]$ is $\sim\frac{1}{3}$ smaller than that $[6.55(7)\times10^{-4}\,\mathrm{kbar}^{-1}]$ in the (101) plane. The small κ can be directly related to the formation of the polymer chain.

As seen from the inset in Fig. 10(b), the extrapolation with the Murnaghan EOS,[49,50] which can be applied in a high-pressure region, for the plots of the $C_{60}\cdots C_{60}$ center-to-center distances in the $(10\bar{1})$ and (101) planes versus pressure, shows that these distances approach each other with an increase in pressure. The center-to-center distance in the (101) plane at 150 kbar is estimated from the extrapolation to be 9.28 Å which is consistent with the distance in the $(10\bar{1})$ plane at 1 bar. This result implies the formation of polymer chains in both planes at 150 kbar. On the other hand, the $C_{60}\cdots C_{60}$ distance in the $(10\bar{1})$ plane is estimated to be 8.95 Å at 150 kbar. Consequently, a 3D anisotropic polymeric phase, with two types of polymer chains, may be realized above 150 kbar. As seen from Fig. 9(d), β decreases straightforwardly up to 53 kbar. This corresponds to the fact that both distances approach each other with an increase in pressure. However, β is expected not to reach to 90° at 150 kbar, judging from the extrapolation for the $C_{60}\cdots C_{60}$ distances. The C-C distances at 150 kbar are expected to be 1.9 Å in the $(10\bar{1})$ plane and 2.6 Å in the (101) plane. The distances realized at 150 kbar should be shorter than the above values because in this analysis the distortion of C_{60} molecule from I_h symmetry is not considered. However, the C-C distance in

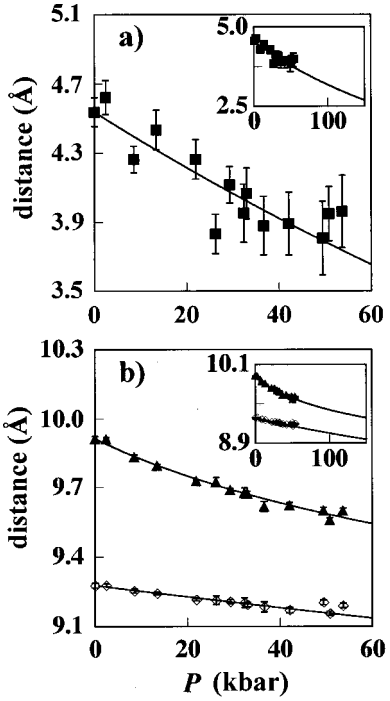

FIG. 10. Plots of (a) the Na···Na distance along the [100] direction in the (010) plane and (b) plots of the center-to-center distances between the C_{60} molecules in the $(10\bar{1})$ and (101) planes vs pressure. ▲ and ◇ refer to the distances in the (101) and $(10\bar{1})$ planes, respectively. Extrapolations with the Murnaghan EOS are shown in (a) and (b).

the (101) plane is still longer than that in the $(10\bar{1})$ plane at 1 bar (2.18 Å). The fact that β is not 90° produces a difficulty in the formation of short C-C contact because of the molecular orientation of C_{60}. Consequently, we present two scenarios: that the 2D polymeric phase of Na_4C_{60} transforms spontaneously to a 3D anisotropic polymer phase above 150 kbar, and that the 2D phase transforms to a 3D isotropic polymer phase ($\beta=90°$) through a structural phase transition for the relaxation of the stress produced at high pressure by the orientations of the C_{60} molecules along the ⟨111⟩ direction in the (101) plane. The crystal structure of the 3D isotropic polymer phase is expected to be bct.

The fitting curve with the Murnaghan EOS for the pressure dependence of V is shown in Fig. 9(e). The atmospheric isothermal bulk modulas K_0 was estimated to be 520(1) kbar from the Murnaghan EOS. The K_0 is larger than those of 1D polymeric Na_2CsC_{60} (280 kbar)[45] and Li_3CsC_{60} (260 kbar).[46] This result can be reasonably explained by the fact that the C_{60} molecules in Na_4C_{60} polymerize two dimensionally, different from 1D polymeric fullerides. The V at 150 kbar predicted from the extrapolation is 1140 Å^3.

As seen from the inset in Fig. 10(a), the Na···Na distance predicted at 150 kbar from the extrapolation with the Murnaghan EOS for the plots of the closest Na···Na distance is 2.7 Å which is much smaller than the sum of van der Waals radius of Na atoms, 4.54 Å.[34] The value is close to the nearest Na···Na distance for the Na_9 cluster in $Na_{9.7}C_{60}$, 2.78 Å,[48] and larger than that for the Na^+ cluster, 2.34 Å.[48] Therefore, the 3D polymeric phase of Na_4C_{60} will be realized through the formation of a Na cluster.

IV. CONCLUSIONS

The temperature dependence of χ_{spin}, ΔH_{pp}, the g factor, and $\Delta H_{pp}/(\Delta g)^2$ estimated from ESR showed a clear change below 100 K. The structural anomaly around 50 K, indicated from the temperature dependence of lattice constants, may be related to the change in the ESR. If the ground state below 50 K is a CDW-type nonmagnetic state, as expected from ESR, the structural change accompanied by the transformation from a polymer to a dimer may be observed in the powder x-ray-diffraction pattern. Though a structural anomaly is indicated around 50 K, definitive evidence for a structural transition, such as the appearance of new Bragg reflections, was not found from the x-ray diffraction.

The pressure dependence of lattice constants showed a smaller κ than those of monomeric and 1D single C-C polymeric fullerides.[41–43,45,46] It was found that the κ of lattice constants was governed by the Na···Na repulsion. The κ of the center-to-center distance between C_{60} molecules in the polymer chain was $\sim\frac{1}{3}$ smaller than that between the κ's in contact with the van der Waals interaction. The formation of two types of polymer chains in Na_4C_{60} around 150 kbar is expected from the extrapolation with the Murnaghan EOS for the pressure dependence of the C_{60}···C_{60} center-to-center distances in $(10\bar{1})$ and (101) planes. Further, the 3D isotropic polymer phase may also be realized through a structural transition. If the 3D polymerized phase of Na_4C_{60} can be realized, the phase should exhibit a metallic behavior and an extremely small $N(\varepsilon_F)$. This phase is very interesting from the viewpoint of a comparative study of the monomeric bct phase (metallic) of Na_4C_{60}, which is realized above 500 K.[23]

ACKNOWLEDGMENTS

The authors acknowledge Y. Iwasa and T. Mitani of JAIST for the opportunity to use Raman equipment. We are grateful to K. Ishii and A. Fujiwara of University of Tokyo, and to Y. Murakami and H. Nakao of KEK-PF, for their valuable discussion in x-ray-diffraction measurements under high pressure. The x-ray-diffraction study was performed under a proposal of KEK-PF (99G032). This work was supported by a Grant-in-Aid (11165227) from the Ministry of Education, Science, Culture and Sports, Japan.

[1] J. Winter and H. Kuzmany, Solid State Commun. **84**, 935 (1992).
[2] Q. Zhu *et al.*, Phys. Rev. B **47**, 13 948 (1993).
[3] P. W. Stephens *et al.*, Nature (London) **370**, 636 (1994).
[4] G. Oszlanyi *et al.*, in *Physics and Chemistry of Fullerenes and Derivatives*, edited by H. Kuzmany, J. Fink, M. Mehring, and S. Roth (World Scientific, Singapore, 1995), p. 323.
[5] O. Chauvet *et al.*, Phys. Rev. Lett. **72**, 2721 (1994).

[6] J. Robert *et al.*, Solid State Commun. **96**, 143 (1995).
[7] M. Kosaka *et al.*, Phys. Rev. B **51**, 12 018 (1995).
[8] V. A. Atsarkin, V. V. Demidov, and G. A. Vasneva, Phys. Rev. B **56**, 9448 (1997).
[9] P. Petit, J. Robert, and J. E. Fischer, Phys. Rev. B **51**, 11 924 (1995).
[10] G. Oszlanyi *et al.*, Phys. Rev. B **51**, 12 228 (1995).
[11] Q. Zhu, D. E. Cox, and J. E. Fischer, Phys. Rev. B **51**, 3966 (1995).
[12] G. Oszlanyi *et al.*, Phys. Rev. B **54**, 11 849 (1996).
[13] M. C. Martin *et al.*, Phys. Rev. B **49**, 10 818 (1994).
[14] G. M. Bendele *et al.*, Phys. Rev. Lett. **80**, 736 (1998).
[15] K. Prassides *et al.*, J. Am. Chem. Soc. **119**, 834 (1997).
[16] Q. Zhu, Phys. Rev. B **52**, R723 (1995).
[17] L. Cristofolini *et al.*, Chem. Commun. (Cambridge), 375 (1997).
[18] G. Oszlanyi *et al.*, Phys. Rev. Lett. **78**, 4438 (1997).
[19] M. de Seta and F. Evangelisti, Phys. Rev. Lett. **71**, 2477 (1993).
[20] Y. Iwasa *et al.*, J. Phys. Chem. Solids **54**, 1795 (1993).
[21] R. F. Kiefl *et al.*, Phys. Rev. Lett. **69**, 2005 (1992).
[22] M. Kosaka *et al.*, Chem. Phys. Lett. **203**, 429 (1993).
[23] G. Oszlanyi *et al.*, Phys. Rev. B **58**, 5 (1998).
[24] O. Zhou and D. E. Cox, J. Phys. Chem. Solids **53**, 1373 (1992).
[25] C. A. Kuntscher, G. M. Bendele, and P. W. Stephens, Phys. Rev. B **55**, R3366 (1997).
[26] M. Knupfer and J. Fink, Phys. Rev. Lett. **79**, 2714 (1997).
[27] M. Fabrizio and E. Tosatti, Phys. Rev. B **55**, 13 465 (1997).
[28] *Atomic and Molecular Physics. Magnetic Properties of Coordination and Organo-Metallic Transition Metal Compounds*, edited by K.-H. Hellwege and O. Madelung, Landolt-Börnstein, New Series, Group II, Vol. 2 (Springer, Berlin, 1966), p. 324.
[29] L. Barbedette *et al.*, in *Physics and Chemistry of Fullerenes and Derivatives*, edited by H. Kuzmany, J. Fink, M. Mehring, and S. Roth (World Scientific, Singapore, 1995), p. 460.
[30] F. Izumi, in *The Rietveld Method*, edited by R. A. Young (Oxford University Press, New York, 1993), p. 236.
[31] T. Yildirim *et al.*, Phys. Rev. Lett. **71**, 1383 (1993).
[32] Y. Kubozono *et al.*, Phys. Rev. B **59**, 15 062 (1999).
[33] P. A. Heiney *et al.*, Phys. Rev. Lett. **66**, 2911 (1991).
[34] A. Bondi, J. Phys. Chem. **68**, 441 (1964).
[35] A. Lappas *et al.*, J. Phys.: Condens. Matter **11**, 371 (1999).
[36] W. I. F. David *et al.*, Nature (London) **353**, 147 (1991).
[37] A. P. Ramirez *et al.*, Phys. Rev. Lett. **69**, 1687 (1992).
[38] D. Arcon *et al.*, Phys. Rev. B **60**, 3856 (1999).
[39] B. Simovic *et al.*, Phys. Rev. Lett. **82**, 2298 (1999).
[40] S. Rouziere *et al.*, Europhys. Lett. **51**, 314 (2000).
[41] T. Yildirim *et al.*, Phys. Rev. B **60**, 10 707 (1999).
[42] O. Zhou *et al.*, Science **255**, 833 (1992).
[43] W. I. F. David and R. M. Ibberson, J. Phys.: Condens. Matter **5**, 7923 (1993).
[44] J. E. Fischer *et al.*, Science **252**, 1288 (1991).
[45] S. Margadonna *et al.*, J. Solid State Chem. **145**, 471 (1999).
[46] S. Margadonna *et al.*, Chem. Mater. **11**, 2960 (1999).
[47] R. D. Shannon, Acta Crystallogr., Sect. A: Cryst. Phys., Diffr., Theor. Gen. Crystallogr. **32**, 751 (1976).
[48] T. Yildirim *et al.*, Nature (London) **360**, 568 (1992).
[49] F. D. Murnaghan, Proc. Natl. Acad. Sci. U.S.A. **30**, 244 (1947).
[50] J. M. Macdonald and D. R. Powell, J. Res. Natl. Bur. Stand., Sect. A **75**, 441 (1971).